Parameter Identification of Nonlinear Ocean Mooring Systems Using the Hilbert Transform

O. Gottlieb

M. Feldman

Faculty of Mechanical Engineering,
Technion—Israel Institute of Technology,
Haifa 32000, Israel

S. C. S. Yim

Ocean Engineering Program,
Department of Civil Engineering,
Oregon State University,
Corvallis, OR 97331

We introduce and demonstrate the applicability of a parameter identification algorithm based on the Hilbert transform to nonlinear ocean mooring systems. The mooring dynamical system consists of a submerged small body and includes a geometrically nonlinear restoring force and a nonlinear dissipation function incorporating both viscous and structural damping. By combining a recently developed methodology with a generalized averaging procedure, parameter estimation from the slowly varying envelope dynamics is enabled. System backbone curves obtained from data generated by numerical simulation are compared to those obtained analytically and are found to be accurate. An example large-scale experiment is also considered.

Introduction

Ocean mooring systems are characterized by a nonlinear restoring force, a structural damping force, and a coupled fluid-structure interaction exciting force (Chakrabarti, 1990). The restoring force includes material discontinuities and geometric nonlinearities associated with large mooring line angles (Bernitsas and Chung, 1990; Gottlieb and Yim, 1992). The hydrodynamic exciting force includes quadratic nonlinearities and periodic components governed by wave-induced viscous drag, radiation damping, and inertial effects. Coupling of degrees of freedom further complicates system behavior. Small body systems (with respect to the flow wavelength) or structures with slender elements do not alter the incident flow, whereas large bodies change the flow field in the vicinity of the body (Sarpkaya and Isaacson, 1981; Chakrabarti, 1987). Consequently, small body systems are typically solved directly due to the explicit form of the exciting force, while large body systems require an approximation of the exciting force or a simultaneous solution of the field-body boundary value problem.

Although the hydrodynamic exciting force of small and large body systems fundamentally differ in their complexity, both systems incorporate similar elements of coupled nonlinear damping and inertial mechanism and equivalently incorporate the nonlinearities of the mooring restoring force and structural damping force. While the nonlinear mooring restoring force can be conveniently derived from a potential function describing a pretensioned geometric configuration, derivation of the exciting force requires knowledge of force coefficients associated with the relative motion of the structure. The force coefficients consist of added masses characterizing the inertial terms and damping coefficients characterizing dissipation due to wave-induced form drag or radiation damping.

The force coefficients are typically deduced from a set of calibration experiments where the structural system parameters are predetermined and the form of exciting force is assumed for given environmental conditions (e.g., a relative motion Morison equation for small-body dynamics in a drag-dominated flow regime). Among the methods employed to extract the coefficients are Fourier averaging or least-squares techniques (Sarpkaya and Isaacson, 1981; Chakrabarti, 1987). Furthermore, spectral-based system identification techniques have been developed to obtain frequency-response functions for wave force calculation on a fixed structure and a nonlinear drift force model (Bendat, 1990).

An alternative method recently developed by the second author to evaluate structural and damping coefficients and frequency response functions for weakly nonlinear vibration systems utilizes the Hilbert transform (Feldman, 1985; 1994a, b). In the past years, the Hilbert transform has been widely used as a signal processing tool (Bendat and Piersol, 1986; Mitra and Kaiser, 1993). The Hilbert transform of a time series will identify existence of a nonlinear component and detect the degree of nonlinearity (Tomlinson, 1987). Examples employing the Hilbert transform in the ocean domain are in the analysis of local properties of sea waves and wave groups (Bitner-Gregersen and Gran, 1983; Hudspeth and Medina, 1988) and in the detection of nonlinear wave buoy motions (Wang and Teng, 1994). Application of the Hilbert transform to both free and forced vibration of mechanical systems enables the instantaneous identification of system parameters based on signal processing of both input and output signal measurements of the dynamical system. Thus, nonlinear frequency-response functions are obtained for both the natural frequency and modal damping.

In this paper, we apply the Hilbert transform method (Feldman, 1994a, b) to results obtained from numerical simulation of a pretensioned small body mooring system (Gottlieb, 1991). The accuracy of the mooring system frequency and damping response curves obtained via the Hilbert transform is verified by comparison with backbone curves obtained analytically for both free (Gottlieb et al., 1994) and forced vibration. We then apply the Hilbert transform to results obtained from a large-scale mooring experiment (Yim et al., 1993). By combining the resulting damping response curve with an approximate curve obtained by a generalized averaging procedure (Sanders and Verhulst, 1985), we obtain estimates for both structural and hydrodynamical mooring system parameters. We close with a discussion on the advantages and limitations of the proposed identification scheme and on directions for future research.

The System Model

The ocean mooring system considered (Fig. 1) is formulated as a single degree of freedom (surge), hydrodynamically

Contributed by the OMAE Division for publication in the JOURNAL OF OFFSHORE MECHANICS AND ARCTIC ENGINEERING. Manuscript received by the OMAE Division, January 3, 1995; revised manuscript received November 29, 1995. Associate Technical Editor: C. Aage.

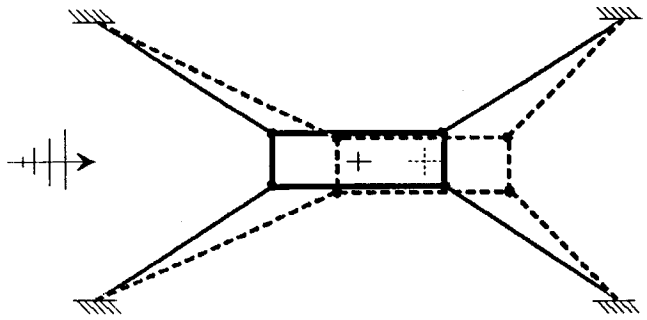

Fig. 1 Mooring assembly

damped and pretensioned nonlinear oscillator (Gottlieb, 1991). In this study, we consider a symmetric four-line restoring force, including a geometric nonlinearity for large-angle motion and neglect the nonlinear convective force. The resulting equation of motion derived from small body theory is

$$m\ddot{X} + c_s\dot{X} + R(X; l_i, l_c, k) = F(\dot{X}, \ddot{X}; c_d, c_a, a, \omega) \quad (1a)$$

where the system mass, structural damping, and mooring line stiffness are m, c_s, and k, respectively. F is the hydrodynamic damping and inertial exciting force, which is formulated as a relative motion Morison equation (Sarpkaya and Isaacson, 1981; Chakrabarti, 1987)

$$F = \frac{\rho}{2} sc_d(U - \dot{X})|U - \dot{X}| + \rho\forall(1 + c_a)\dot{U} - \rho\forall c_a\ddot{X} \quad (1b)$$

where c_a and c_d are added-mass and drag coefficients, respectively; ρ is water mass density; s and $\forall$ are the body drag projected area and displaced volume, respectively; U is the horizontal particle velocity based on linear wave theory

$$U = a\omega \frac{\cosh k(z + h)}{\sinh kh} \cos \omega t, \quad \omega^2 = gk \tanh kh \quad (1c)$$

where a, ω, and k are the incident wave amplitude, cyclic frequency, and wave number, respectively; z and h denote body and water depth, respectively; and g is the gravitational acceleration. R is the elastic cable restoring force

$$R = k\left\{4X + l_c\left[(2b - L)\frac{l_1 - l_2}{l_1 l_2} - 2X\frac{l_1 + l_2}{l_1 l_2}\right]\right\} \quad (1d)$$

where l_i ($i = 1, 2$) and l_c are the in-situ mooring line and initial pretensioned lengths, respectively,

$$l_{1,2} = \left[\left(b - \frac{L}{2} \pm x\right)^2 + \left(d - \frac{B}{2}\right)^2\right]^{1/2} \quad (1e)$$

and L and B are the body length and beam, b and d are the horizontal and vertical mooring anchor coordinates, respectively.

Rearranging and scaling ($x = X/(d - B/2)$) the system (1) results in the following:

$$\ddot{x} + D(\dot{x}; \gamma, \delta) + R(x; \alpha, \beta, \tau) = F(t; \mu, \omega) \quad (2a)$$

where F is the external excitation

$$F = -\kappa\mu\omega^2 \sin \omega t \quad (2b)$$

D is the normalized dissipation function

$$D = \gamma\dot{x} - \delta(u - \dot{x})|u - \dot{x}|, \quad u = \kappa\omega \cos \omega t \quad (2c)$$

R is the normalized restoring force

$$R = \alpha\left\{x - \tau\left[\frac{\beta + x}{\sqrt{1 + (\beta + x)^2}} - \frac{\beta - x}{\sqrt{1 + (\beta - x)^2}}\right]\right\} \quad (2d)$$

and α, β, τ are the nondimensional stiffness, geometrical mooring configuration, and pretension parameters

$$\alpha = \frac{4k}{m + \rho\forall c_a}, \quad \beta = \frac{2b - L}{2d - B}, \quad \tau = \frac{l_c}{2d - B} \quad (2e\text{–}g)$$

γ, δ are structural and hydrodynamical damping parameters

$$\gamma = \frac{c_s}{m + \rho\forall c_a}, \quad \delta = \frac{\rho(2d - B)sc_d}{4(m + \rho\forall c_a)} \quad (2h, i)$$

and $\kappa\mu$ is the forcing parameter

$$\kappa = \frac{2a}{2d - B}\frac{\cosh k(z + h)}{\sinh kh}, \quad \mu = \frac{\rho\forall(1 + c_a)}{m + \rho\forall c_a}. \quad (2j, k)$$

Note that the system degree of nonlinearity is controlled by the geometric mooring parameter β, the pretension parameter τ, and the nonlinear damping parameter δ. The pretension parameter $\tau \le \frac{1}{2}\sqrt{(1 + \beta^2)}$ corresponds to $l_c \le l_0 = \sqrt{((b - 0.5L)^2 + (d - 0.5B)^2)}$. The strongest nonlinearity is obtained for taut ($\tau = 0.5$) right-angle mooring ($\beta = 0$), whereas the weakest nonlinearity is found for small angles ($\beta \gg 1$) and large pretension ($\tau \ll \frac{1}{2}\sqrt{(1 + \beta^2)}$).

Identification of Mooring System Parameters Using the Hilbert Transform

Recently, nonlinear frequency and damping response backbone curves have been successfully obtained by applying the Hilbert transform to data generated by simulation of weakly nonlinear free and forced vibration systems (Feldman 1994a, b). For convenience, we summarize the main results in the Appendix and demonstrate that this procedure is valid for the processing of signals with nonoverlapping spectra (Coulon, 1986). In this section we demonstrate the applicability of the method for parameter identification of the ocean mooring system model (2).

The Hilbert transform is first applied to free vibration simulation results generated by numerical integration of the system (2) with $\alpha = \beta = 1$, $\tau = \sqrt{2}/2$, $\gamma = \delta = 0.05$, $\kappa = 0$. The instantaneous envelope is depicted as $A(t)$ with the response $y(t)$ in Fig. 2(a). Implementation of the algorithm described in the Appendix for free vibration ($z(t) = 0$ in (19)) results in the instantaneous natural frequency response ($A(f_0)$) and instantaneous equivalent damping coefficient ($A(\dot{h}_0)$) of the system shown in Fig. 2(b). A low-frequency filtration of the natural frequency and damping response functions enables construction of the nonlinear backbone curves for both restoring force and dissipation functions (Fig. 2(b)). Note that the degree of nonlinearity is portrayed by the angle of the backbone curves and that application of the algorithm to simulation results of a linearized oscillator will yield vertical backbones anticipated by analysis of a linear mechanical system (Feldman and Braun, 1993). The offset for the zero amplitude of the damping response curve $A(h_0) = 0$ is half the value of the structural damping parameter $h_0 = \gamma/2$, which in Fig. 2(b) ($\gamma = 0.05$) is $h_0 = 0.025$. The offset for zero amplitude of the frequency response ($A(f_0) = 0$) corresponds to the equivalent linearized natural frequency. This can be shown by expanding the restoring force $R(x)$ in (2d) about the unique stable fixed point at the origin

$$R_L(x) = \omega_0^2 x = \alpha[1 - 2\tau(1 + \beta^2)^{-3/2}]x \quad (4)$$

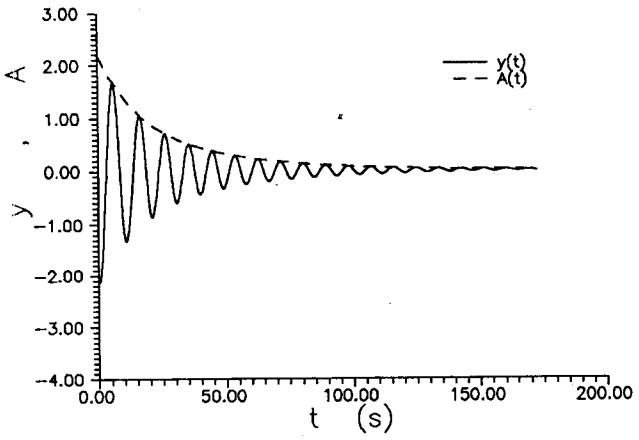

(a) Response $y(t)$ and Hilbert envelope $A(t)$

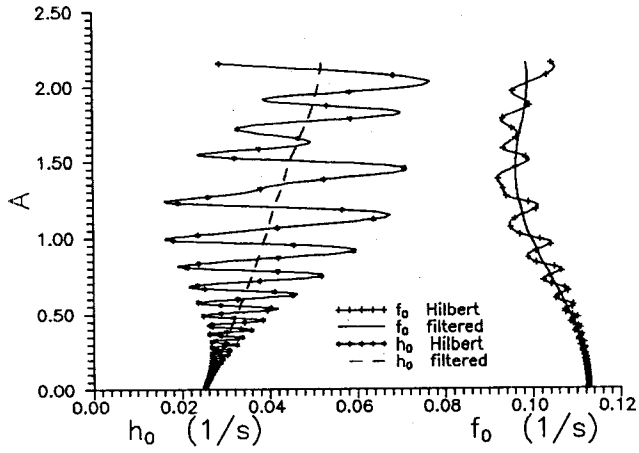

(b) Natural frequency response $A(f_0)$ and damping response $A(h_0)$

Fig. 2 Free vibration ($\alpha = \beta = 1$, $\tau = \sqrt{2}/2$, $\gamma = \delta = 0.05$, $\kappa = 0$)

Note that the linearized natural frequency for a taut mooring configuration reduces to $\omega_0^2 = \alpha\beta^2/(1 + \beta^2)$, corresponding to $\omega_0 = \sqrt{1/2}$ or $f_0 = 0.1125$ for the values of $\alpha = \beta = 1$ as depicted by the free vibration of Fig. 2(b). Measurement of the mooring line angles (β) and pretension (τ) enable calculation of the mooring stiffness parameter (α) from (4). Consequently, the added-mass coefficient (c_a) can be obtained given calibration data of the cable stiffness (k).

In order to apply the Hilbert transform to forced vibration simulation results, we assume a weakly nonlinear formulation for the dissipation function (2c). Thus, an equivalent linear damping over a wave period is obtained.

$$D_L(\dot{x}) = \gamma\dot{x} - \bar{\delta}(u - \dot{x}) = \gamma\dot{x} - \frac{8\delta}{3\pi}|u|(u - \dot{x}) \quad (5)$$

Consequently, the wave-structure interaction coupling in (2c) can be separated resulting in the input/output relationship required by the quasi-linear formulation of (19). Substitution of (5) for (2c) and rearranging (2a) results in the following:

$$\ddot{x} + \Gamma\dot{x} + R(x; \alpha, \beta, \tau) = K\cos(\omega t + \Phi) \quad (6a)$$

where

$$\Gamma = \gamma + \frac{8\delta\kappa\omega}{3\pi} \quad (6b)$$

$$K = \kappa\omega^2\sqrt{\mu^2 + \left(\frac{8\kappa\delta}{3\pi}\right)^2}, \quad \Phi = \tan^{-1}\left(\frac{3\pi\mu}{8\kappa\delta}\right) \quad (6c, d)$$

and $R(x)$ remains as in (2d). The Hilbert transform is applied to forced vibration simulation results generated by numerical integration of (6) with $\alpha = \beta = 1$, $\tau = \sqrt{2}/2$, $\gamma = \delta = 0.05$, $\mu = 1$, $\omega = 0.65$. The instantaneous envelope $A(t)$ with the response $y(t)$ generated by a harmonic exciting force ($\kappa = 0.24$) is shown in Fig. 3(a). Implementation of the algorithm described in the foregoing for various forcing amplitudes ($\kappa = 0.14, 0.24, 0.33$) results after a low-pass filtration in discrete values for the instantaneous natural frequency response ($A(f_0)$) and instantaneous equivalent damping ($A(h_0)$) coefficients of the system which are shown in Fig. 3(b). An alternative input function which can be used in a controlled experimental environment is excitation by a "chirp" function defined by $F(t) = K\cos[\Omega(t)t + \Phi]$ where $\Omega(t) = \omega(0.1 + 2t/t_{max})$. This form of excitation $z(t)$, depicted in Fig. 4(a), enables an amplitude-varying response function $y(t)$ and Hilbert envelope $A(t)$ in Fig. 4(b). Consequently, continuous forms of both frequency and damping response backbone curves are obtained from a single controlled experimental run, as is shown in Fig. 3(b). The filtered frequency response backbone curve for forced vibration ($A(f_0)$ in Fig. 3(b)) was found to be identical to that obtained for small amplitudes ($A < 0.5$) in free vibration ($A(f_0)$ in Fig. 2(b)), and differed only slightly for larger amplitudes.

Verification of System Backbone Curves Obtained From Simulated Results

In this section we compare the backbone curves obtained from numerically simulated data to those obtained analytically

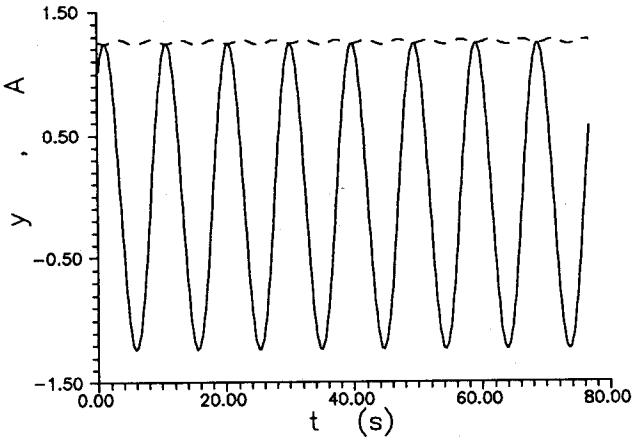

(a) Response and Hilbert envelope ($\kappa = 0.24$)

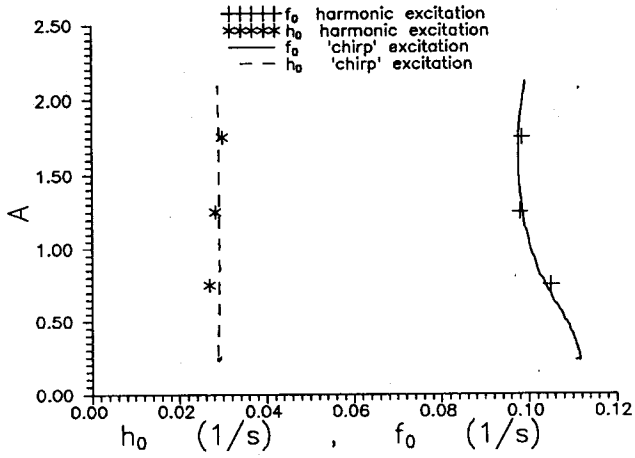

(b) Natural frequency and damping frequency response to harmonic excitation ($\kappa = 0.14, 0.24, 0.33$) and to a "chirp" excitation ($\kappa = 0.24$)

Fig. 3 Forced vibration ($\alpha = \beta = 1$, $\tau = \sqrt{2}/2$, $\gamma = \delta = 0.05$, $\mu = 1$, $\omega = 0.65$)

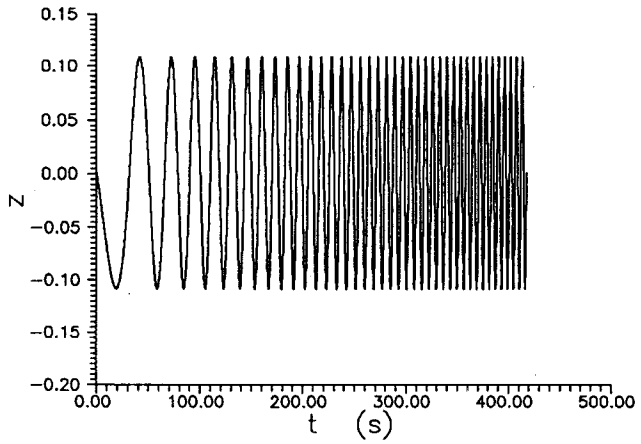

(a) "Chirp" exciting force $z(t)$

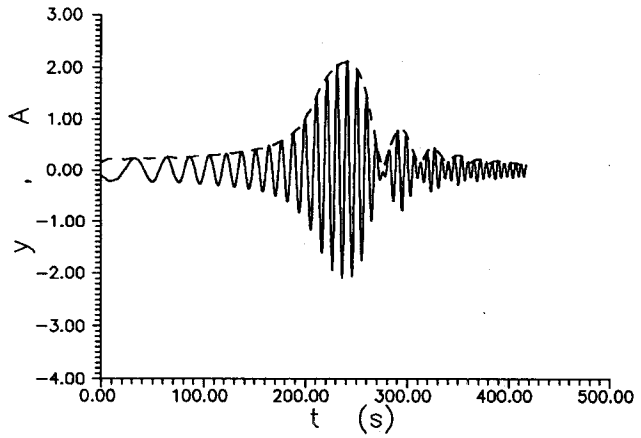

(b) Response and Hilbert envelope

Fig. 4 Forced vibration ($\alpha = \beta = 1$, $\tau = \sqrt{2}/2$, $\gamma = \delta = 0.05$, $\mu = 1$, $\kappa = 0.24$, $\omega = 0.65$)

in order to verify the accuracy of the identification algorithm. Our analysis consists of investigation of the influence of each nonlinear component of the system (2). The natural frequency of the system (f_0) can be obtained analytically by direct integration of the system Hamiltonian phase plane ($\gamma = \delta = 0$). The total energy of the system can be written as

$$H = \tfrac{1}{2}\dot{x}^2 + V(x) \tag{7a}$$

where the potential $V(x) = \int R(x)dx$ is

$$V(x) = \alpha\left\{\frac{x^2}{2} - \tau[\sqrt{1 + (\beta + x)^2} + \sqrt{1 + (\beta - x)^2}]\right\} \tag{7b}$$

Consequently, as the natural period of the system can be integrated (Gottlieb, 1991), a closed-form analytical backbone curve for the natural frequency can be obtained

$$T = 4\int_0^A \frac{dx}{\sqrt{2[V(x_0) - V(x)]}} = \frac{2\pi}{\omega_0} = \frac{1}{f_0} \tag{8}$$

where $V(x_0)$ is a function of initial conditions. Comparison of results obtained from the Hilbert transform for weak damping ($\gamma = \delta = 0.01$) and zero tension ($\tau = \frac{1}{2}\sqrt{(1 + \beta^2)}$) with those obtained analytically for $\beta = 0$ and $\beta = 1$ are shown in Fig. 5(*a*). Note the Hilbert transform natural frequency oscillates about the analytical results for large amplitudes and is sensitive to the degree of nonlinearity. However, the low-pass filter of the Hilbert envelope coincides with the theoretical backbone obtained from (8).

In order to compare the damping coefficient via the Hilbert transform with results from an approximate perturbation approach, we restrict our analysis to weak hydrodynamic damping of a taut small angle mooring system ($\beta > 1$) or a system with large pretension ($\tau < 0.5\sqrt{(1 + \beta^2)}$). The natural frequency of the linearized restoring force was determined in (4), and a higher-order expansion enables derivation of a cubic term in the restoring force. Thus, the weakly nonlinear mooring system is written as

$$\begin{aligned}\ddot{x} + \omega_0^2 x &= \epsilon f(x, \dot{x}, t) \\ &= \epsilon[-\hat{\alpha}_3 x^3 - \hat{\gamma}\dot{x} \\ &\quad + \hat{\delta}(u - \dot{x})|u - \dot{x}| - \hat{\kappa}\mu\omega^2 \sin \omega t]\end{aligned} \tag{9a}$$

where

$$\alpha_3 = \alpha\tau(1 - 4\beta^2)(1 + \beta^2))^{-7/2} \tag{9b}$$

and $(\alpha_3, \gamma, \delta) = \epsilon(\hat{\alpha}_3, \hat{\gamma}, \hat{\delta})$, $\epsilon \ll 1$; u is defined in (2*c*).

Free Vibration. For small damping values ($\gamma, \delta \ll 1$) and weakly nonlinear mooring ($\alpha_3 \ll 1$), we employ a generalized averaging method (Sanders and Verhulst, 1985) to obtain the slowly varying envelope evolution equations of the weakly nonlinear system (9). The evolution equations for the amplitude and phase are obtained for the unforced system ($\kappa = 0$) by

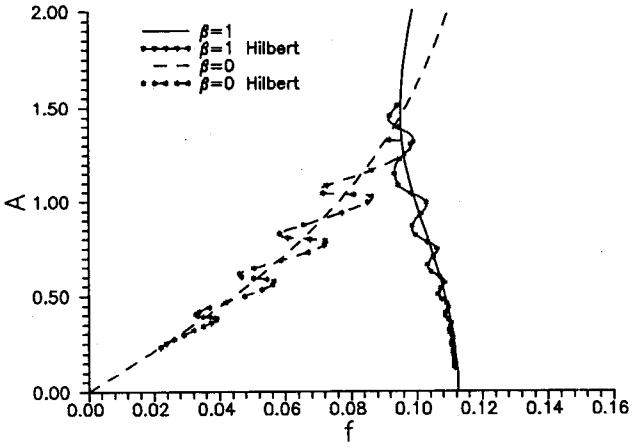

(a) Free vibration [$(\beta, \tau) = (0, 1/2), (1, \sqrt{2}/2)$, $\kappa = 0$]

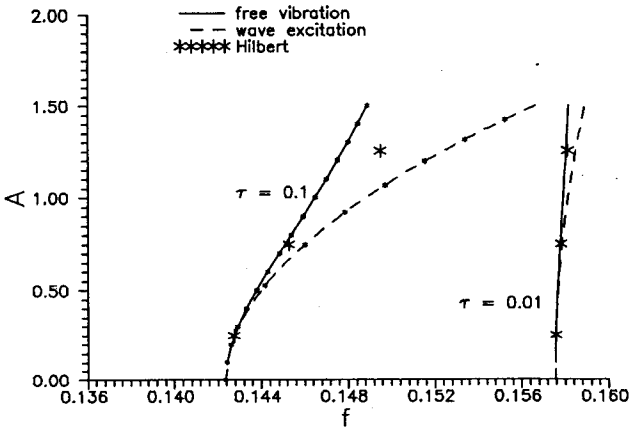

(b) Forced vibration [$\beta = 0$, $\tau = (0.01, 0.1)$, $\kappa = (0.0225, 0.1125)$, $\omega = 0.65$]

Fig. 5 Comparison of analytical and Hilbert transform natural frequency response curves ($\alpha = 1$, $\gamma = \delta = 0.01$)

averaging over the natural period ($2\pi/\omega_0$) where the solution form to $O(\epsilon)$ is $x = A\cos(\omega_0 t + \psi)$ for $\epsilon \ll 1$.

$$\dot{A} = -\left[\frac{\gamma}{2}A + \frac{4\delta\omega_0}{3\pi}A^2\right]$$

$$\dot{\psi} = \frac{3\alpha_3}{8\omega_0}A^2 \qquad (10a, b)$$

Note that (10a) is a function of A only and can be solved in closed form to yield an approximate expression for the instantaneous envelope, after which the phase can be also integrated (Nayfeh and Mook, 1979).

$$A(t) = \frac{A_0 \exp\left(\frac{-\gamma t}{2}\right)}{1 + \left(\frac{8\omega_0\delta}{3\pi\gamma}\right)A_0\left[1 - \exp\left(\frac{-\gamma t}{2}\right)\right]} \qquad (11)$$

Comparison of the instantaneous envelope via the Hilbert transform and (11) are identical for small values of γ, $\delta < 0.1$ (Gottlieb et al., 1994).

Forced Vibration. We now consider the evolution equations for the slowly varying amplitude and phase for the forced system. These are obtained by averaging over the forcing period ($2\pi/\omega$) where the solution form to $O(\epsilon)$ is $x = A\cos(\omega t + \psi)$ for $\epsilon \ll 1$.

$$\dot{A} = -\frac{\gamma}{2}A + \frac{\kappa\mu\omega}{2}\cos\Psi - \frac{\delta\omega^2}{2\pi}(I_S\cos\theta + I_C\sin\theta)$$

$$A\dot{\Psi} = -\frac{\Delta}{2}A + \frac{3\alpha_3}{8\omega}A^3 - \frac{\kappa\mu\omega}{2}\sin\Psi - \frac{\delta\omega^2}{2\pi}(I_C\cos\theta - I_S\sin\theta) \qquad (12a, b)$$

where Δ is a detuning parameter

$$\Delta = \frac{\omega^2 - \omega_0^2}{\omega} \qquad (12c)$$

and

$$\begin{pmatrix} I_S \\ I_C \end{pmatrix} = \int_0^{2\pi/\omega} [\kappa\cos\omega t + A\sin(\omega t + \Psi)]\left|\kappa\cos\omega t + A\sin(\omega t + \Psi)\right|\begin{pmatrix}\sin\omega t \\ \cos\omega t\end{pmatrix} dt \qquad (12d, e)$$

Solution of (12) can be obtained numerically and the steady-state slowly varying frequency response can be obtained by calculating the fixed points ($\dot{A}, \dot{\psi} = 0$) of (12) (Gottlieb, 1991). However, the frequency response backbone of (12) can be obtained from the undamped ($\gamma = \delta = 0$) unforced ($\kappa = 0$) steady state of (12), which yields the following quadratic amplitude frequency relationship:

$$A^2 = \frac{4}{3}\left|\frac{\omega^2 - \omega_0^2}{\alpha_3}\right| \qquad (13)$$

Comparison of the approximate frequency response from (13) to that obtained by applying the Hilbert transform to simulations of (2) for a strong geometric nonlinearity ($\beta = 0$) with moderate ($\tau = 0.1$) and strong ($\tau = 0.01$) pretension and weak damping ($\gamma = \delta = 0.01$) are shown in Fig. 5(b). For convenience, we plot the respective theoretical frequency response curves obtained from (8). The results portrayed in Fig. 5(b) demonstrate the coincidence of the Hilbert obtained frequency response point for weak excitation ($\kappa = 0.0225$) with the theoretical results from the approximate wave excitation analysis (13) and the exact free vibration analysis (8). An increase in the magnitude of wave excitation ($\kappa = 0.1125$) demonstrates the sensitivity of the Hilbert obtained forced vibration results to the degree of nonlinearity ($\tau = 0.1$). However, it should be emphasized that the validity of the approximate frequency response (13) is itself sensitive to the degree of the nonlinearity, as are all perturbation-based approximations.

Analysis of Experimental Results

We demonstrate the application of the algorithm presented on results obtained from a large-scale experiment done at the Oregon State University Wave Research Lab (Yim et al., 1993). The experimental model consisted of a submerged sphere (diameter = 0.4572 m) moored at a right angle ($\beta = 0$) to the walls of a two-dimensional basin with moderate pretension ($\tau = 0.344$). The submerged sphere ($z = -0.97155$ m, $h = 2.7432$ m) was subjected to both free and forced vibration tests, which were done by plucking the model in still water ($\kappa = 0$) and exciting it via harmonic wave excitation ($\kappa, \omega > 0$). Single-degree-of-freedom motion was ensured by constraining the sphere, which was manufactured with delron bearings, to move along an aluminum rod. System displacement measurements were done via string pots connected to the sphere and wave excitation was measured by an array of resistance-type wave-gages located fore and aft of the model.

Free Vibration. The Hilbert envelope ($A(t)$) obtained from an example free vibration test demonstrates an almost linearlike decay characteristic of Coulomb damping (Nayfeh and Mook, 1979) due to the constrained sphere motion in Fig. 6(a). The filtered backbone curves for both frequency and damping response are presented in Fig. 6(b). While the content of Coulomb-like damping is evident by the hyperboliclike shape of the damping response curve $A(h_0)$ in Fig. 6(b) (Feldman, 1994a), an equivalent instantaneous damping force, $D(\dot{y}) = 2h_0(A)\dot{y}$, depicted in Fig. 7($b$) enables estimation of the magnitudes of both the Coulomb and structural damping components. Furthermore, the equivalent instantaneous restoring force, $R(y) = \omega_0^2(A)y$, in Fig. 7(a) also reveals the linear behavior of the restoring force for large amplitudes. Note that due to the characteristics of the Coulomb damping, the frequency and damping responses cannot be obtained for small amplitudes ($y < 0.03$, $\dot{y} < 0.05$).

Based on the linear behavior of the equivalent instantaneous damping force for large velocities ($\dot{y} > 0.1$) in Fig. 7(b), the hyperbolic structure of the experimental free vibration damping response can be approximated by considering a weakly nonlinear mooring system (9a), where the perturbation consists of an equivalent linear damping component modified with an additional threshold for Coulomb damping

$$\ddot{x} + \omega_0^2 x = -\alpha_3 x^3 - \Gamma\dot{x} - \nu\,\mathrm{sgn}(\dot{x}) \qquad (14)$$

where ν is the magnitude of the Coulomb damping, sgn ($\dot{x}$) is the sign of the body velocity ($\dot{x}$), Γ is an equivalent linear damping coefficient describing both structural and hydrodynamical damping, and α_3 is defined in (9b). Following the procedure outlined in the previous section results in the evolution equations for the slowly varying amplitude and phase

$$\dot{A} = -\left[\frac{\Gamma}{2}A + \frac{2\nu}{\pi\omega_0}\right] = -\left[\frac{\Gamma}{2} + \frac{2\nu}{\pi\omega_0}\frac{1}{A}\right]A$$

$$\dot{\Psi} = \frac{3\alpha_3}{8\omega_0}A^2 \qquad (15a, b)$$

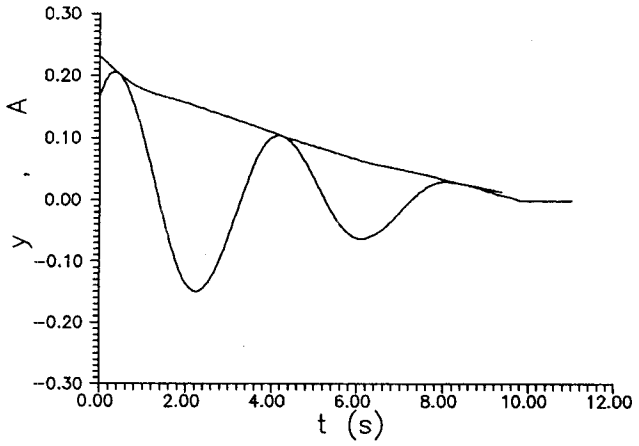

(a) Free vibration response and Hilbert envelope,

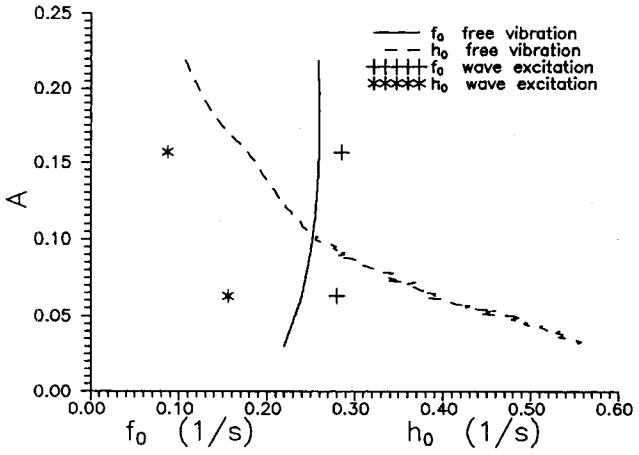

(b) Natural frequency and damping frequency response to free vibration ($\kappa = 0$), and harmonic excitation ($\kappa = 0.012, 0.031$, $\omega = 1.698$)

Fig. 6 Experimental free and forced vibration ($\beta = 0$, $\tau = 0.344$)

We note that (15a) is only a function of the dissipation mechanisms and that a quasi-linear approximation for the Hilbert damping response can be obtained in a similar manner to yield

$$\dot{A} = -[h_0(A)]A \tag{16}$$

Consequently, by equating the right-hand sides of (15a) and (16), an approximate relationship for the hyperbolic structure can be obtained

$$A(h_0) = \frac{4}{\pi\omega_0}\frac{\nu}{2h_0 - \Gamma} \tag{17}$$

We now return to Fig. 6(b) and calculate both equivalent linear damping and Coulomb damping coefficients ($\Gamma = 0.062$, $\nu = 0.071$) based on a constant (mean) natural frequency ω_0 ($\bar{f}_0 = 0.225$).

We note that the magnitudes of both structural (γ) and hydrodynamic (δ) damping components cannot be obtained under free vibration, and thus consider the resultant linear damping coefficient as an upper bound for structural damping (i.e., $\gamma_{max} = \Gamma = 0.062$). Furthermore, although the offset for zero amplitude of the frequency response is not available in Fig. 6(b) due to the Coulomb damping characteristics ($A < 0.03$), an approximate value for the mass parameter ($\alpha = 6.406$) can be obtained from (4) based on an estimated natural frequency ($\bar{f}_0 = 0.225$). Consequently, an added-mass coefficient $c_a = 0.5025$ can be obtained from (2e) ($k = 234.1$ N/m, $m = 48.06$ kg, $\rho\forall = 50.04$ kg), corresponding to the classical value of the added mass of a submerged sphere (Chakrabarti, 1987).

Forced Vibration. We now turn to preliminary results obtained from an example forced vibration test under harmonic excitation. A normalized free surface ($z(t) = \eta/(d - 0.5B)$, η measured) and model output response ($y(t) = y^*(t)/(d - 0.5B)$, y^* measured) are presented in Fig. 8(a, b). Generation of the free surface was achieved by harmonic excitation of the basin piston-type wavemaker (for a small amplitude $a = 0.034$ m and frequency $\omega = 1.6982$ rad/s corresponding to $T = 3.7$ s). However, the required steady-state response of the model included weak re-reflections (from the beach and wavemaker itself), imposing a slight variability of the input amplitude at the free surface (Fig. 8a). Additional sources of variability are due to higher-order effects produced by the prescribed motion of the wavemaker itself. We note that the depth parameter $kh = 1.0378$ obtained from the linear dispersion relation (1c) corresponds to an intermediate depth wave, and that the diffraction parameter $kB = 0.173$ corresponds to a small body excitation regime ($kB < 1.25$) or to a small body size/wavelength = $0.0275 < 0.2$. The input exciting force was calculated by multiplying the normalized free surface by a factor F_0 ($F_0 = \mu[\cosh k(z + h)/\sinh kh]\omega^2 = 2.959$) based on linear wave theory where $\mu = 1.027$ was calculated from ($2k$). The Hilbert transform of input and output results of two tests ($\kappa = 0.012, 0.031$) yields two pairs of discrete values of filtered frequency and damping responses depicted in Fig. 6(b). We note that the natural frequency response values $A(f_0)$ are slightly higher than

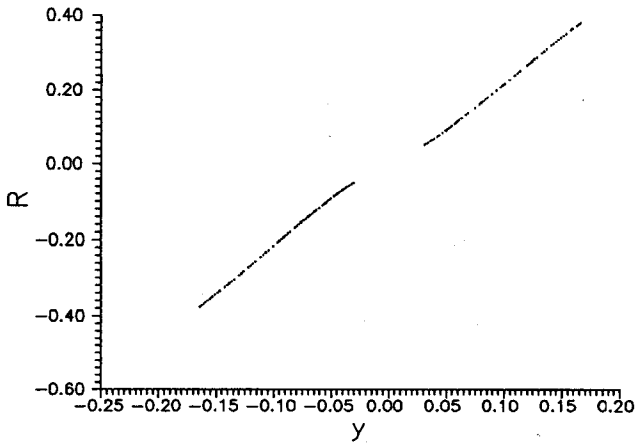

(a) Restoring force $R(y) = \omega_0^2(A)y$

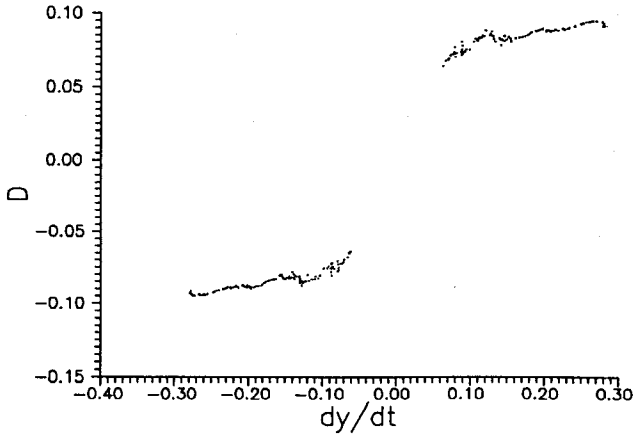

(b) Damping force $D(\dot{y}) = h_0(A)\dot{y}$

Fig. 7 Experimental instantaneous free vibration force responses

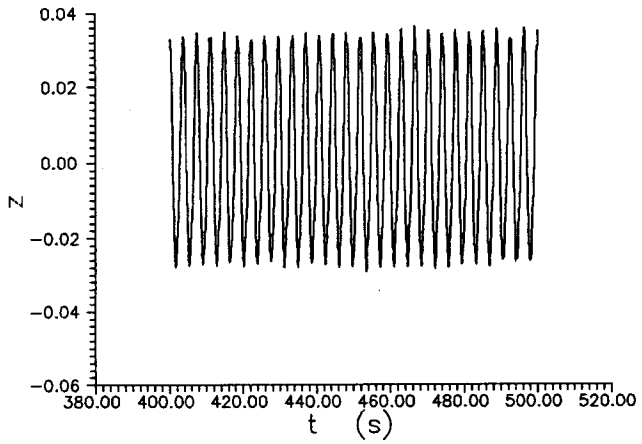

(a) Normalized free surface $z(t) = \eta(t)/(d - 0.5B)$

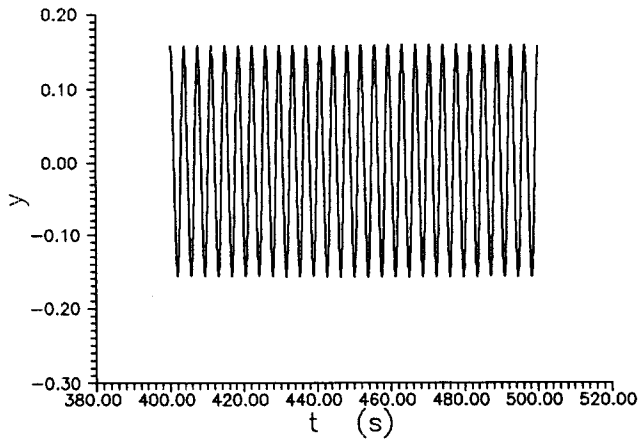

(b) Normalized sphere surge $y(t) = y(t)/(d - 0.5B)$

Fig. 8 Experimental input and output measurements ($\beta = 0$, $\tau = 0.344$, $\kappa = 0.031$, $\omega = 1.698$)

that obtained from free vibration. However, the magnitude of the damping frequency response $A(h_0)$ is much smaller than that obtained from the free vibration test. The large difference in the damping frequency response is due to a much smaller magnitude of the Coulomb damping component, which varied harmonically under wave excitation. In free vibration, the normal force and contact area between the sphere and constraining rod were constant, whereas under wave excitation, the normal force and effective contact area were smaller as they varied with the periodic lift force. Furthermore, recall that the results are obtained from a Hilbert transform of an input measured at the free surface and not by direct measurement of the exciting force at the location of the body. The variability the free surface measurement is depicted by the noisy content of the input signal spectra demonstrating existence of additional harmonics (Fig. 9(*a*)) versus the smooth spectra of the response (Fig. 9(*b*)).

In order to estimate the dissipation parameters, we consider the evolution equations under wave excitation and obtain an approximate expression for the possible hyperbolic structure including structural damping, wave drag, and Coulomb damping

$$A(h_0) = \frac{4}{\pi\omega} \frac{\nu^*}{2h_0 - \Gamma^*} \tag{18a}$$

where ν^* is a modified Coulomb damping and Γ^* consists of both structural and linearized wave drag components

$$\Gamma^* = \gamma + \frac{8\delta\kappa\omega}{3\pi} \tag{18b}$$

Substitution of the amplitude and damping frequency data pairs $(A(h_0))$ into (18) and solving two equations for the two unknown damping coefficients (ν^*, Γ^*) results in estimated values for the modified Coulomb damping coefficient ($\nu^* = 0.027$) and for the equivalent structural and wave drag coefficient ($\Gamma^* = 0.0815$). Knowledge of an upper bound for the structural damping coefficient ($\gamma_{max} = 0.06$) from free vibration enables calculation of a lower bound for the wave drag parameter from (18*b*) ($\delta_{min} = 0.48$). Consequently, the wave drag coefficient is calculated from (2*i*), resulting in $c_d = 0.28$. We note that this value is a lower bound for the drag coefficient and its sensitivity is a function of the structural and Coulomb damping estimates. The Reynolds and Keulegan-Carpenter numbers for this test based on a maximum calculated sphere velocity (0.4 m/s) were Re = 1.2 10^5 and KC = 3.25. We note that the corresponding drag coefficient for a sphere based on the equivalent steady flow value (cf., Newman, 1977) is $c_d = 0.43$. Furthermore, drag and added-mass coefficients obtained for a submerged sphere in a sinusoidally oscillating fluid (Sarpkaya, 1975) for corresponding KC value are $c_d \approx 0.25$ and $c_a \approx 0.55$.

Summary and Conclusions

We have demonstrated the applicability of a parameter identification algorithm based on the Hilbert transform for nonlinear ocean mooring systems. By combining a recently developed methodology based on the Hilbert transform of both input and output time domain data with a generalized averaging procedure, parameter identification from the slowly varying envelope dynamics is enabled for both free and forced vibration. Free vibration calibration results in parameter identification of the system natural frequency

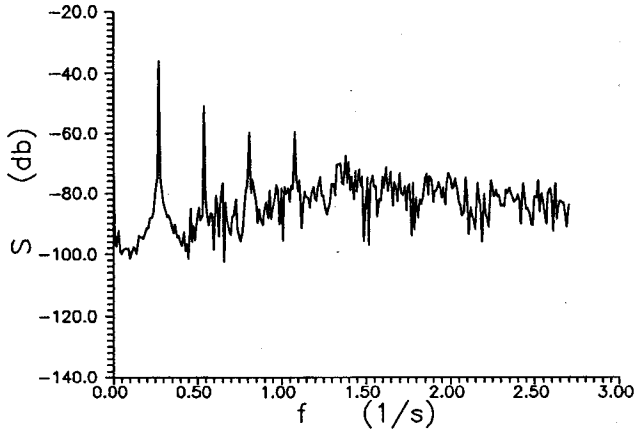

(a) Normalized free surface

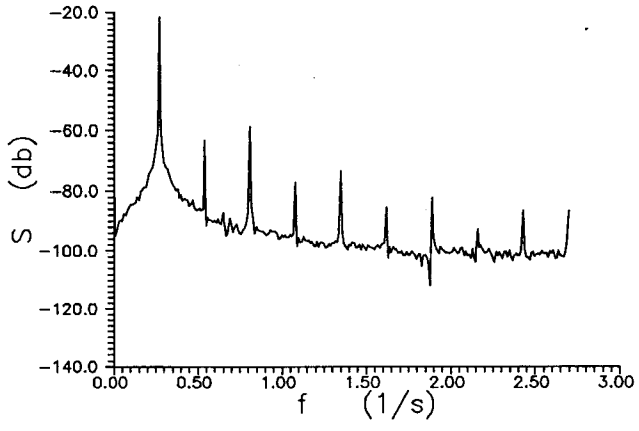

(b) Sphere surge

Fig. 9 Experimental input and output spectra ($\beta = 0$, $\tau = 0.344$, $\kappa = 0.031$, $\omega = 1.698$)

and damping parameters independent of the equivalent system mass. Consequently, the added-mass and structural damping coefficients can be estimated. Forced vibration analysis requires, in addition to simultaneous measurements of input and output, knowledge of the mass and structural damping parameters in order to estimate the wave drag coefficient.

Verification of the nonlinear system backbone curves obtained from the Hilbert transform of simulated data was performed by comparison with analytical solutions of a mooring system for a given geometry and pretension condition. The calculated results were found to be identical to those obtained analytically for free vibration and compared well with those obtained by an approximate perturbation approach under wave excitation. Parameter estimates were obtained from a large-scale experiment by combining the resulting backbone curves with those obtained by the averaging procedure describing the mooring system envelope dynamics. The influence of data measurement, variability of system input, and the complexity introduced by an additional nonlinear dissipation mechanism were also revealed in the analysis of experimental results.

In closing we remark that a quantitative estimate of mooring system parameters is enabled from the response backbone curves obtained via the Hilbert transform method combined with a theoretical description of the slowly varying envelope dynamics. Furthermore, while error analysis is identical to that of other spectral-based identification schemes, the Hilbert transform algorithm enables nonlinear parameter estimates from a minimal data set. We note that while this identification scheme is straightforward for single-degree-of-freedom motion, coupled multi-degrees-of-freedom response requires further investigation, particularly in the case of nonlinear coupling of fluid-structure interaction terms.

Acknowledgments

This study was supported in part by the United States Office of Naval Research (Grant No. 00014-92-J-1221), the Fund for Promotion of Research at the Technion and the Israel Ministries of Science & Technology and Immigrant Absorption, for which the authors are grateful.

References

Bendat, J. S., and Piersol, A. G., 1986, *Random Data-Analysis and Measurement Procedures,* John Wiley & Sons, New York, NY.

Bendat, J. S., 1990, *Nonlinear System Analysis and Identification,* Wiley-Interscience, New York, NY.

Bernitsas, M. M., and Chung, J. S., 1990, "Nonlinear Stability and Simulation of Two-Line Ship Towing and Mooring," *Applied Ocean Research,* Vol. 11, pp. 153–166.

Bitner-Gregersen, E. M., and Gran, S., 1983, "Local Properties of Sea Waves Derived From a Wave Record," *Applied Ocean Research,* Vol. 5, pp. 210–214.

Chakrabarti, S. K., 1987, *Hydrodynamics of Offshore Structures,* Springer, Berlin, Germany.

Chakrabarti, S. K., 1990, *Nonlinear Methods in Offshore Engineering,* Elsevier, Amsterdam, The Netherlands.

Coulon, F., 1986, *Signal Theory and Processing,* Arthech House.

Feldman, M., 1985, "Investigation of the Natural Vibrations of Machine Elements Using the Hilbert Transform," *Soviet Machine Science,* Vol. 2, pp. 44–47.

Feldman, M., 1994a, "Nonlinear System Vibration Analysis Using the Hilbert Transform, Part I: Free Vibration," *Mechanical Systems and Signal Processing,* Vol. 2, pp. 119–227.

Feldman, M., 1994b, "Nonlinear System Vibration Analysis Using the Hilbert Transform, Part II: Forced Vibration," *Mechanical Systems and Signal Processing,* Vol. 3, pp. 243–249.

Feldman, M., and Braun, S., 1993, "Analysis of Typical Nonlinear Vibration Systems by Using the Hilbert Transform," *Proceedings, XIth International Modal Analysis Conference,* pp. 799–805.

Gottlieb, O., 1991, "Nonlinear Oscillations, Bifurcations and Chaos in Ocean Mooring Systems," Ph.D. thesis, Oregon State University, Corvallis, OR.

Gottlieb, O., Feldman, M., Yim, S. C. S., and Braun, S., 1994, "Estimation of Nonlinear Ocean Mooring System Parameters via the Hilbert Transform," *Proceedings, 25th Israel Mechanical Engineering Conference,* Haifa, Israel, pp. 393–395.

Gottlieb, O., and Yim, S. C. S., 1992, "Nonlinear Oscillations, Bifurcations and Chaos in a Multi-Point Mooring System With a Geometric Nonlinearity," *Applied Ocean Research,* Vol. 14, pp. 291–257.

Hudspeth, R. T., and Medina, J. R., 1988, "Wave Group Analysis by the Hilbert Transform," *Proceedings 21st Coastal Engineering Conference,* Spain, pp. 884–898.

Mitra, S. K., and Kaiser, J. F., 1993, *Handbook for Digital Signal Processing,* Wiley-Interscience, New York, NY.

Nayfeh, A. H., and Mook, D. T., 1979, *Nonlinear Oscillations,* John Wiley & Sons, New York, NY.

Newman, J. N., 1977, *Marine Hydrodynamics,* MIT Press, Cambridge, MA.

Sanders, J. A., and Verhulst, F., 1985, *Averaging Methods in Nonlinear Dynamics,* Springer, New York, NY.

Sarpkaya, T., 1975, "Forces on Cylinders and Spheres in a Sinusoidally Oscillating Fluid," ASME *Journal of Applied Mechanics,* Vol. 42, pp. 32–37.

Sarpkaya, T., and Isaacson, M., 1981, *Mechanics of Wave Forces on Offshore Structures,* Van Nostrand-Reinhold, New York, NY.

Tomlinson, G. R., 1987, "Developments in the Use of the Hilbert Transform for Detecting and Quantifying Nonlinearity Associated With Frequency Response Functions," *Mechanical Systems and Signal Processing,* Vol. 1, No. 2, pp. 151–171.

Wang, H. T., and Teng, C. C., 1994, "Nonlinear Aspects of the Motion Behavior of Directional Wave Buoys," *Proceedings, 13th International Conference of OMAE,* Vol. I, ASME, Houston, TX, pp. 11–18.

Yim, S. C. S., Myrum, M. A., Gottlieb, O., Lin, H., and Shih, I-M., 1993, "Summary and Preliminary Analysis of Nonlinear Oscillations in a Submerged Mooring System Experiment," Oregon State University, Ocean Engineering Report No. OE-93-03.

APPENDIX

Parameter Identification Using the Hilbert Transform

Following Feldman (1994a, b), we consider the following quasi-linear system:

$$\ddot{y} + 2h_0(A, \Psi)\dot{y} + \omega_0^2(A, \Psi)y = \frac{z(t)}{m} \tag{19}$$

where $\omega_0(A, \Psi)$ and $h_0(A, \Psi)$ are amplitude and phase-dependent natural frequency and equivalent damping coefficients, respectively, and $z(t)$ is an external excitation. Furthermore, we require that both coefficients ω_0^2 and h_0 be functions of a slowly varying amplitude $A(\epsilon t)$ and phase $\Psi(\epsilon t)$, so that $y(t)$ and the coefficient functions $f(\epsilon t)$, ($f(\epsilon t) = \omega_0^2(\epsilon t)$ or $h_0(\epsilon t)$), are signals with nonoverlapping spectra (Coulon, 1986). Thus, application of the Hilbert transform ($\mathbf{H}[x(t)]$) to both sides of (19) results in a differential equation for the complex analytic signal forms for both input and output as the Hilbert transform of $f(\epsilon t)g(t)$ can be decomposed as $\mathbf{H}[f(\epsilon t)g(t)] = f(\epsilon t)\mathbf{H}[g(t)]$, where $f(\epsilon t) = \omega_0^2$ and $g(t) = y(t)$ or $f(\epsilon t) = h_0$ and $g(t) = dy(t)/dt$.

Substitution of the output $Y(t) = A(t)\exp[j\psi(t)]$ and input excitation $Z(t) = B(t)\exp[j\phi(t)]$ into (19) results in a complex ordinary differential equation. Separating real and imaginary parts and rearranging terms results in the following:

$$\ddot{Y} + 2h_0(A, \Psi)\dot{Y} + \omega_0^2(A, \Psi)Y = \frac{Z}{m} \tag{20}$$

where the frequency and damping response curves are

$$\omega_0^2 = \dot{\psi}^2 - \frac{\ddot{A}}{A} + \frac{2\dot{A}^2}{A^2} + \frac{\dot{A}\ddot{\psi}}{A\dot{\psi}} + \frac{1}{m}\left(P - \frac{\dot{A}Q}{A\dot{\psi}}\right)$$

$$h_0 = -\frac{\dot{A}}{A} - \frac{\ddot{\psi}}{2\dot{\psi}} + \frac{1}{m}\left(\frac{Q}{2\dot{\psi}}\right) \tag{21a, b}$$

and

$$\frac{Z(t)}{Y(t)} = P(t) + jQ(t) = \frac{zy + \tilde{z}\tilde{y}}{y^2 + \tilde{y}^2} + j\frac{\tilde{z}y - z\tilde{y}}{y^2 + \tilde{y}^2} \tag{22a, b}$$

Note that $y(t)$, $z(t)$ are the output and input signals, respectively, and $\tilde{y}(t)$, $\tilde{z}(t)$ are their real valued Hilbert transforms: $Y(t) = y(t) + j\tilde{y}(t)$, $Z(t) = z(t) + j\tilde{z}(t)$. Parameter identification can also be obtained for free vibration ($z(t) = 0$) in (19) where ω_0^2 and h_0 are independent of the mass parameter (m in (20)).